Coded-aperture, multi-wavelength Raman spectroscopy for ethanol detection in biological samples

S.T. McCain, M.E. Gehm, Y. Wang, N.P. Pitsianis, D.J. Brady

Duke University Fitzpatrick Center for Photonic and Communications Systems and Department of Electrical and Computer Engineering, Box 90291, Durham, NC 27708
stm2@duke.edu

Abstract

Optical diagnostics in biological materials are hindered by fluorescence and scattering. We have developed a multimodal, multiplex, coded-aperture Raman spectrometer to detect alcohol in a lipid tissue phantom solution.

Keywords: Optical biosensor, Raman spectroscopy, multiplex sensing.

1. Introduction

Raman spectroscopy is a powerful diagnostic tool due to its high specificity and possibility for *in vivo* applications[1]. At the same time, its very weak signal strength and incoherent scattering properties make it a challenging signal to detect. In biological systems where cells scatter strongly and fluoresce, this detection problem is compounded even further. We have designed and constructed a multimodal multiplex Raman spectrometer which uses coded aperture spectroscopy to have a large collection area and multi-wavelength excitation to better detect signals in the presence of fluorescence. While such spectrometers have been studied before[2], ours is novel due to its static design and use of a 2-dimensional coding pattern. We have demonstrated the detection of ethanol in solutions of a lipid tissue phantom. At high lipid concentrations, our instrument detects Raman signatures which are not observable in a research grade instrument. We have also reconstructed multi-wavelength data of ethanol and blood mixtures.

2. Background and Theory

2.1. Coded Aperture Spectroscopy

In bio-photonic applications, diffuse, incoherent sources are large in size due to scattering. The average spectral density, S(λ), averaged over some finite area is a measurement of interest. In dispersive spectrometers, this measurement is made by observing the intensity on the detector plane, I(x'), with an aperture function, A(x), and linear dispersion on the detector plane, α, which can be described as:

$$I(x') = \int A(x)S((x-x')/\alpha)dx \qquad (1)$$

Equation 1 has an inherent ambiguity between aperture position and spectral channel. With a slit this ambiguity is broken by providing a delta function as the aperture function, however this is done with a reduction in throughput. This throughput-resolution tradeoff is avoided with an aperture function of the form

$$A(x) = \sum_j \delta(x - x_j) \qquad (2)$$

giving a modified detector intensity of

$$I(x') = \sum_j S((x_j - x')/\alpha) \qquad (3)$$

Thus combinations of the spectral density are measured at every detector, allowing for a system with high resolution and throughput. Deconvolution to estimate the spectral density is possible in this case, however the conditionality of this transformation is very poor. By measuring combinations of codes, a greater family of transformations is possible, with some being very well conditioned. This can be described by

$$I(i,x') = \sum_j S((x_{i,j} - x')/\alpha) \qquad (4)$$

Through the inversion of Equation 4, i shifted spectral estimates are obtained. Thus the spectra can either be imaged in the x direction or these spectra can be shifted and summed to obtain an average spectrum. The mask codes used are from the Hadamard matrices, a square matrix of 1's and -1's which has orthogonal rows and is well-conditioned. To implement the -1's, one row has openings for the -1's, and its

corresponding detector row is subtracted from the detector row corresponding to a row having openings at the 1's. Thus the aperture pattern is rectangular in shape for square apertures.

2.2. Multi-Wavelength Raman Spectroscopy

The wavelength of light scattered inelastically from molecular species can shifted due to energy coupling to the internal vibrational modes of the scattering species. Such frequency shifts result in a discrete array of sharp lines corresponding to harmonic modes of the molecule. This spectral shift is generally referred to as the "Stokes" shift or the "Raman" effect. Raman spectroscopy may be used to identify the presence of a target molecule, to analyze the structure and/or densities of molecular species, and/or for other purposes. However, fluorescence produced by elastic scattering and/or stray light obscures the Raman portion of the spectrum.

Shifted Excitation Raman Difference Spectroscopy ("SERDS") may be used to reduce interference from fluorescence and stray light by shifting the frequency of a laser light that is impinged on a specimen. The Raman bands are generally shifted in response to a shift in excitation frequency, and the broad background fluorescence and stray light are generally much less affected by the excitation frequency shift. SERDS generally involves a subtraction of two spectra obtained from two different (shifted) excitation frequencies. The subtraction can result in a derivative spectrum that may reduce the background and fluorescence spectra[3].

However, SERDS may not sufficiently reduce fluorescence and stray light in all environments. For example, Raman spectroscopy may be more difficult in diffuse media, such as biological tissue, because the Raman effect may be obscured by a high level of incoherent fluorescence spectra and/or by the diversity of molecules and the associated Raman signals that may be present in the media.

A spectral impulse response is used to make a mathematical distinction between a non-Raman signal (e.g., the component of a spectrum that can be attributed to non-Raman scattering) and the Raman signal (e.g., the component of a spectrum that can be attributed to Raman scattering). Both spectral components include sub-components that are linear and non-linear with respect to the exciting wavelengths. However, the linear components are generally stronger than the non-linear components. The linear terms are described by an implulse response. The non-Raman spectrum, S_{NR}, generated by a linear transformation of the exciting intensity is expressed as follows:

$$S_{NR}(\nu) = \int h_{NR}(\nu, \nu')S_e(\nu')d\nu' \qquad (5)$$

where $S_e(\nu)$ is the exciting signal as a function of optical output frequency ν; h_{NR} is the non-Raman impulse response and ν' is an exciting frequency. The distinguishing feature of the Raman and the non-Raman signals is that the Raman impulse response is typically shift invariant in the exciting field, while the non-Raman impulse response is not shift invariant. The term "shift invariant" means that the Raman impulse response is a function only of the difference between the observed frequency and the exciting frequency, e.g., $h_R(\nu, \nu') = h_R(\nu - \nu')$. Therefore, the Raman spectrum is expressed as follows:

$$S_R(\nu) = \int h_R(\nu - \nu')S_e(\nu')d\nu' \qquad (6)$$

The total inelastic scattered spectrum from a source is the sum of the non-Raman and the Raman terms.

An array of individually laser sources that can be modulated can be used to implement a coded Raman spectrometer system. Assuming that the line width of all of the lasers is the same, ($\gamma(\nu)$), but that each source has a different center wavelength (ν_l), the exciting spectrum is expressed as follows:

$$S_e(\nu) = \sum_{l}^{N} \gamma(\nu - \nu_l) \qquad (7)$$

For relatively small shifts in the frequency of the exciting spectrum, it is assumed that the non-Raman signal is independent of the exciting wavelength, in which case:

$$\int h_{NR}(\nu, \nu')\gamma(\nu' - \nu_l)d\nu' \approx S_{NR}(\nu) \qquad (8)$$

The spectroscopy system is used to estimate molecular densities from the Raman signal. The Raman spectrum is estimated as follows:

$$S_R(\nu) = \int h_R(\nu - \nu')\gamma(\nu')d\nu' \qquad (9)$$

3. System Design

For work in tissue, the near-infrared (NIR) region is attractive due to the low photon absorption and availability of high performance CCD detectors in this wavelength range. Excitation at 808nm provides reduced tissue fluorescence and produces Raman peaks of ethanol at 870-930nm. The system is built around a CCD camera from Santa Barbara Instruments Group (SBIG), with a 765x510 pixel detector cooled by a single-stage Peltier cooler. In the Fig. 1 the complete system is shown. The camera was chosen

due to its low cost, ~$1500, 16-bit digitization, and compact form factor. Typical bench top laboratory Raman spectrometers utilize multi-stage cooling and scientific-grade CCDs which dramatically increase the cost of a system. With our aperture coding and multi-wavelength excitation, the goal is to have a system that can have good performance in the presence of noise associated with a higher temperature detector and lower grade CCDs.

Fig. 1 Photograph of assembled system with cover off

The optical system is shown in Fig. 2. Due to the isotropy of Raman scattering, a low f/#, 2.1, system was custom designed, which combined with the large input aperture of the coding mask, ~2mm x 1mm, allows for a high etendue of the entire system. The aperture mask consists of lithographically patterned chrome on quartz. An N=32 Hadamard code with 36 x 36 μm apertures allows for a system resolution of ~1 nm which is matched to the spectral width of the Raman ethanol peaks, also ~ 1nm FWHM. The rectangular aspect ratio of the mask stems from the row doubling in order to implement codes with negative values. To keep the system compact, short focal lengths are used to keep the lens diameters under 1". A volume phase holographic (VPH) grating of 1200 lpmm yields high diffraction efficiencies (>80%) over the wavelengths and angles present in the system. The system described yields a spectral range of 850-950 nm.

The excitation source consists of 4 semiconductor diode lasers, with peak CW powers of ~100 mW, and spectral output of 0.5 nm FWHM. The lasers are mounted on a copper block on top of a Peltier cooler to allow for temperature tuning of the lasers between ~803-810 nm. The laser diodes have a band-pass filter with transmission from 800-820 nm to suppress out of band spontaneous emission and a lens to form a small spot ~100 um x 100 um on the sample of interest.

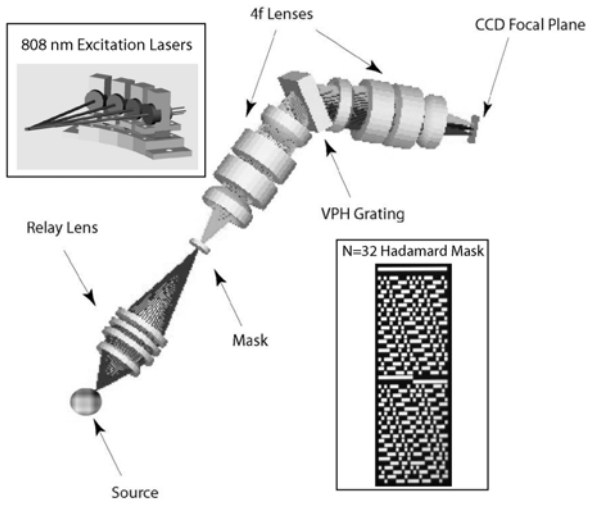

Fig. 2 Optical layout, laser assembly, and aperture mask

4. Data Processing

Multiple processing steps are required to go from the raw data of the CCD to a reconstructed spectrum. A reconstruction with a xenon discharge lamp provides all the fixed calibration data needed to characterize the spectrometer. As seen in Equation 1, the detector reads a convolution of the aperture pattern and the source spectrum. Thus, for a discharge lamp with very narrow peaks, a sharp mask image is created for each spectral peak as shown in Fig 3. By analyzing the image of these masks, it is possible to correct for the so-called "smile" distortion inherent in dispersive spectrometers with low f/#'s. The rows of CCD that correspond to rows of the mask are then found, and the data can be binned into 2N rows where N is the order of the mask. The complementary rows are then subtracted forming a N x M data matrix, where M is the number of CCD columns. The data is then inverted using the following equation:

$$H_{nxn} \times S(\lambda - \Delta_i)_{nxm} = X_{nxm} \qquad (10)$$

where H is the n x n Hadamard matrix, $S(\lambda - \Delta_i)$ is the n x m matrix of shifted spectra, and X is the n x m binned and subtracted CCD values. A non-negative least squares algorithm calculates the reconstructed data set for each column. The shifted spectra are then aligned, and summed, with a reconstructed spectrum of a xenon discharge lamp shown in Fig. 3.

To reconstruct multi-wavelength data, the following equation is inverted to find the signal S_R:

$$m = F_1 S_{NR} + F_2 S_R \quad (11)$$

The matrices F1 and F2 are formed using the knowledge that the SNR signal shifts with excitation wavelength and the SNR is not shifted with each excitation. The m matrix is composed of the reconstructed spectra at different excitation wavelengths. A calibration step with pure ethanol in a scattering solution is done to deduce the shift of the excitation wavelengths.

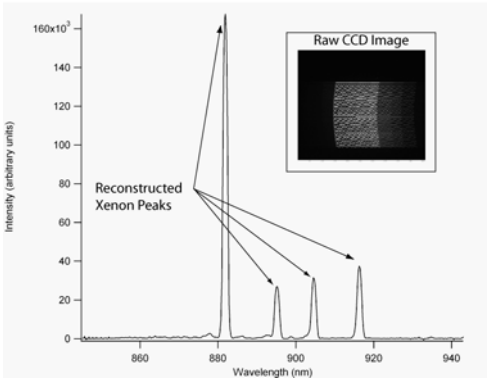

Fig. 3 Reconstructed xenon pen lamp spectrum with corresponding detector image

5. Results and Conclusions

To analyze the performance of the device, liquid samples of varying concentrations of ethanol, water, and a lipid tissue phantom are prepared. Raman spectra taken with one laser diode at 808 nm are shown in Fig. 4. When we compare this data to scans

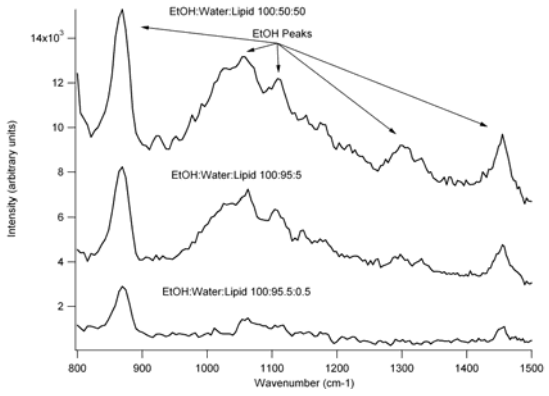

Fig. 4 Single-wavelength reconstructed spectra at varying lipid concentrations spaced for visual separation only (lipid concentration increases vertically)

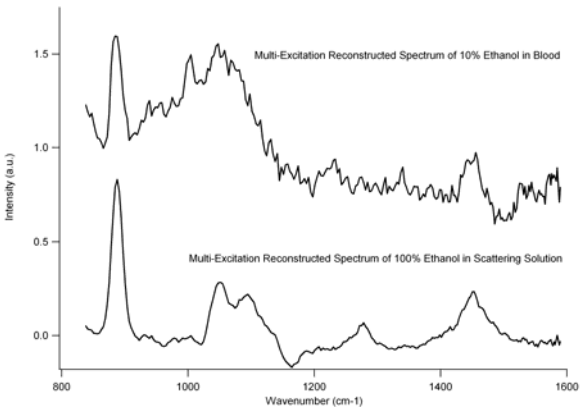

Fig. 5 Multi-wavelength reconstructions of 10% blood in ethanol (top) and 100% ethanol in a microsphere solution (bottom) spaced for visual separation only

taken with a commercial system, we find that our system exhibits a stronger ethanol signal at higher lipid concentrations. We think this is a result of our system being optimized for larger, more diffuse sources. The higher lipid concentrations provide enhanced scattering to enlarge the spatial extent of the Raman photons. To test the multi-wavelength operation of the system, samples of 10% ethanol in blood are prepared and scans are taken at 4 different wavelengths, 803.4 nm, 804.8 nm, 806.0 nm, and 808.6 nm. The 4 scans are combined into 1 reconstructed Raman spectrum through the inversion described earlier. The spectra for 10% ethanol in blood and 100% ethanol in a scattering solution of microspheres are shown in Fig. 5. The two strong peaks of ethanol are clearly shown in the reconstructed spectrum. With enhanced processing and a optimization of the wavelength shift, these signals can be improved. These results show promise for a high sensitivity tissue Raman chemical sensor in scattering, fluorescent media and a higher performance system is under development.

6. References

[1] EB Hanlon et al., "Prospects for in vivo Raman Spectroscopy," *Phys. Med. Biol*. Vol. 45, p. R51-R59 (2000).

[2] Hammaker et al., "Recent developments in Hadamard transform Raman spectrometry," in Raman and Luminescence Spectroscopies in Technology II, F. Adar, J.E. Griffiths, Proc. SPIE Vol. 1336, p. 124-134 (1990).

[3] S.E.J. Bell, E.S.O. Bourguignon, and A. Dennis, "Analysis of luminescent samples using subtracted shifted raman spectroscopy," *Analyst*, Vol. 123, no. 8, p. 1729-1734 (1998).